

Growth crystallography of $\text{Bi}_{12}\text{SiO}_{20}$ single crystals solidified by a floating zone method

SENLIN FU, HIROYUKI OZOE*

Institute of Advanced Material Study, Kyushu University, Kasuga Koen 6-1, Kasuga Fukuoka 816, Japan

Relations between the growth directions of $\text{Bi}_{12}\text{SiO}_{20}$ (BSO) single-crystal rods solidified by a floating zone method and the pulling parameters were studied using an X-ray back-reflection Laue technique. It was found that when a platinum wire is used as a seed, the growth direction of the produced BSO single-crystal rod is related to the pulling rate. Statistically, the probability of the growth direction approaching $\langle 011 \rangle$, $\langle 112 \rangle$ or $\langle 001 \rangle$ appears to increase in this order with increase of the pulling rate. In addition when a BSO crystal is used as a seed, the growth direction of the produced BSO crystal rod has the same orientation as the seed crystal if the pulling rate is less than 30 mm h^{-1} . If the pulling rate is higher than 30 mm h^{-1} , the growth appears to incline mostly to $\langle 112 \rangle$ if the seed orientation is near $\langle 011 \rangle$ or $\langle 111 \rangle$ but far from $\langle 001 \rangle$, or to $\langle 001 \rangle$ if the seed orientation is near $\langle 001 \rangle$ but far from both $\langle 011 \rangle$ and $\langle 111 \rangle$. The angle of inclination increases with the pulling rate, and also with the difference in angle between the orientation of seed crystal and $\langle 112 \rangle$ or $\langle 001 \rangle$. The facet morphology of the BSO single-crystal rod is related to its growth direction. The cross-section of the BSO single-crystal rod grown along $\langle 001 \rangle$ is an octagon with tetrad-rotational symmetry, that grown along $\langle 011 \rangle$ is an ellipsoid with diad-rotational symmetry, and that along $\langle 111 \rangle$ is a hexagon with triad-rotational symmetry. The cross-sections of the BSO single-crystal rods grown in other directions are not regular, because there is no clear symmetry.

1. Introduction

Bismuth silicon oxide, $\text{Bi}_{12}\text{SiO}_{20}$ (BSO), is an outstanding photorefractive material that has attracted increased attention with a view to application in optical information processing and recording components because of its high response speed and good sensitivity [1–5].

Single crystals of BSO have a body-centred cubic structure (bcc, space group $I23$ [6] and are normally grown by the Czochralski method from stoichiometric melts. The reported deficiencies in BSO crystals appear to be due to the characteristics of the Czochralski growth process [3, 5, 7]. For example, impurities dissolved from a crucible wall may be introduced into the matrix of the grown crystal [7]. On the other hand, a floating zone method does not produce such deficiencies, and it offers the possibility of growing single-crystal rods and fibres [8], which can be used directly in optical devices without mechanical working, such as cutting and polishing.

In the present study, the relations between the pulling parameters and the crystallographic orientations (i.e. growth directions) of single-crystal rods of BSO produced by a floating zone method were systematically investigated using an X-ray back-reflection

Laue technique. This provides operational guides as to which growth directions should be selected for various optical devices. It also provides useful guides for $\text{Bi}_{12}\text{GeO}_{20}$ (BGO) and $\text{Bi}_{12}\text{TiO}_{20}$ (BTO) because of their similar structural characteristics.

2. Experimental procedures

Single-crystal growth was accomplished by the infrared-heated floating zone method described previously [8]. Bismuth oxide (Bi_2O_3) of 99.99% purity (powder, $1\text{--}2 \mu\text{m}$) and silicon oxide (SiO_2) of 99.99% purity (powder, $0.8 \mu\text{m}$), made by Johnson Matthey Inc., were thoroughly mixed together in a stoichiometric ratio of 6:1. These powders were mixed with about 5 wt% deionized water at room temperature, then pressed into a cylindrical rod of 6.5 mm (diameter) \times 68 mm (length). After drying for 1 d at room temperature, the rod was sintered at 500°C for 8 h, and then at 515°C for 7 h, 530°C for 5 h, 550°C for 5 h, 580°C for 5 h, and finally at 618°C for 5 h. By X-ray diffraction and the relevant quantitative analysis [9], the concentration of the γ -phase (bcc) in the source rod after this series of sintering processes was measured as 96.98 wt% [10]. To avoid

* Author to whom all correspondence should be addressed.

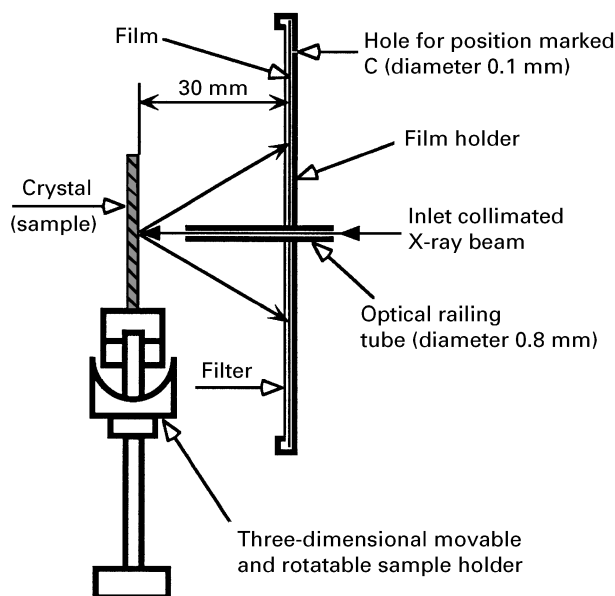


Figure 1 Schematic representation of the back-reflection Laue camera.

contamination, no chemical binders were used in the above processes. Single crystals were produced directly from this sintered powder rod.

Crystal structure was measured by X-ray diffraction. An X-ray back-reflection Laue camera, fitted with a three-dimensional movable and rotatable sample holder and the corresponding parallelometer and angulometer, was used to determine the growth directions of single-crystal rods. The system is schematically illustrated in Fig. 1. The collimated primary X-ray beam enters through an optical railing tube (inside diameter 0.8 mm) in the centre of the film and falls on the crystal surface placed 30 mm from the film. The diffracted beams from the crystal pass through a filter and fall on the film. To obtain accurate orientation of the crystal rod, it must be adjusted so that its axis is parallel to the line joining the centre of the hole of the inlet X-ray beam and the position marked C in the film-holding plate with an error of less than $\pm 0.5^\circ$. The perpendicularity between the film and the inlet X-ray beam is automatically fixed. The accuracy of determination of growth directions of crystal rods by this method is within $\pm 2^\circ$. The error in determining the growth direction change in the same crystal rod was within $\pm 0.5^\circ$ or within $\pm 0.2^\circ$ if diffraction points near the edge of the film were chosen for comparison.

The Laue pattern and metalloscopy were employed to identify the facet morphologies of the grown crystal rods.

3. Experimental results

3.1. Structure of grown BSO crystal rods

Fig. 2 shows the X-ray diffraction pattern of the powder made of the BSO crystal rod grown at 16.8 mm h^{-1} from the sintered powder rods by using a platinum wire as seed. A similar pattern was obtained for that grown at 106.8 mm h^{-1} . To avoid the

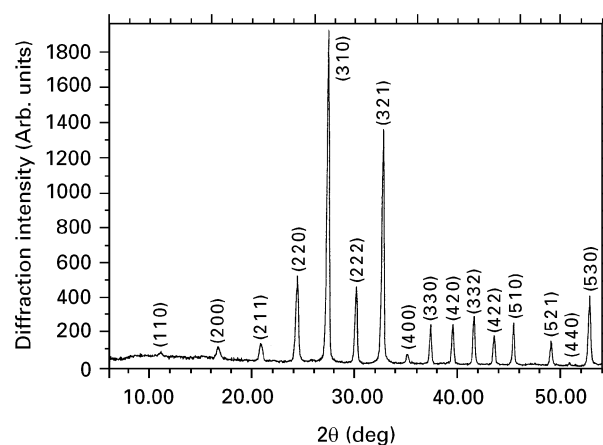


Figure 2 X-ray diffraction patterns of powders made of BSO crystal rods grown at 16.8 mm h^{-1} .

crystallization of the δ -phase (fcc), the temperature of the melt was controlled at less than 935°C for both cases. The grown BSO crystals consisted entirely of the pure body-centred cubic (bcc) γ -phase, although they were pulled at very different rates. The lattice constants of the crystals grown at 16.8 and 106.8 mm h^{-1} were determined as 1.01068 and 1.01077 nm, respectively, by the method described previously [11]. The small difference between these two lattice constants may be attributed to crystal defects in the latter crystal due to the high pulling rate.

3.2. Determination of the growth direction

Fig. 3a is a typical back-reflection Laue pattern of a grown BSO crystal rod, 2.3 mm in diameter. The pulling rate is 16.8 mm h^{-1} . The centre of the pattern was determined from the point of intersection of line A–B with the perpendicular line through point C. By use of a Greninger chart [12], Wulff's stereographic net and stereographic projections of cubic structure, the growth direction of the crystal rod was calculated as shown in Fig. 3b and c. To avoid a possible shape change in the photographic print, the calculation was made directly from the film of the Laue pattern. The growth directions of all crystals were determined in the same way.

3.3. Growth direction with a platinum seed

The growth directions of BSO single-crystal rods produced by using the same platinum wire (0.5 mm diameter) as a seed, at 16.8, 68.8 and 106.8 mm h^{-1} , are shown in Fig. 4. Here we omitted the direction differences in a single orientation group, e.g. the difference between [001], [010] and [100] in the $\langle 001 \rangle$ group, due to the crystal symmetry. The diameters of all grown crystal rods were controlled in the range of $2.30 \pm 0.05 \text{ mm}$. Ten crystal rods were tested for each pulling rate. From the data plotted in Fig. 4, the probability of the preferred growth direction $\langle 011 \rangle$ appears to decrease with increasing pulling rate. The most probable growth direction appears to be $\langle 112 \rangle$ for 68.8 mm h^{-1} and $\langle 001 \rangle$ for 106.8 mm h^{-1} . The

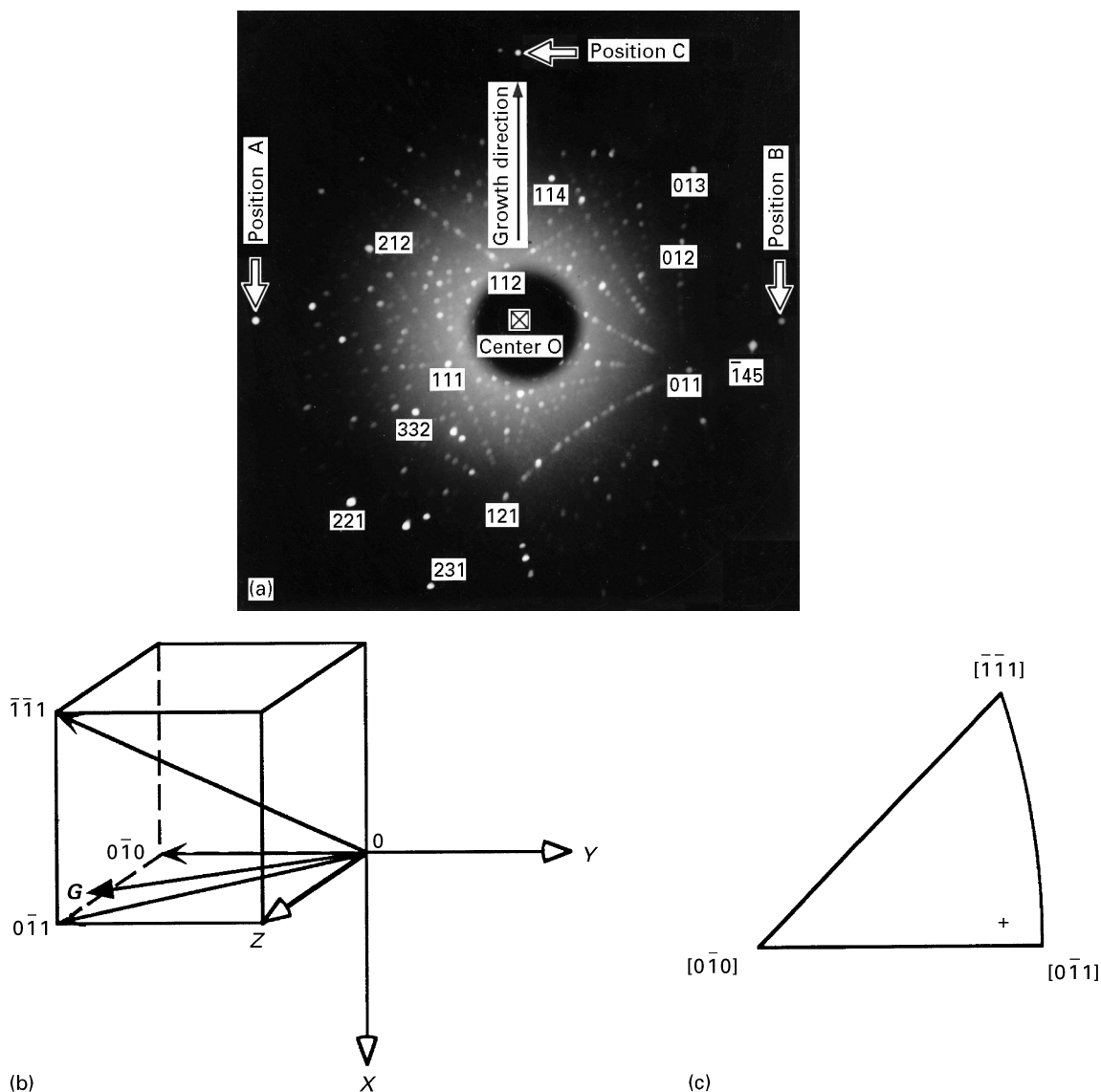


Figure 3 (a) X-ray back-reflection Laue pattern of a BSO crystal grown from a platinum seed at 16.8 mm h^{-1} . (b) Crystal growth direction (vector G) shown in a cubic unit cell, determined from the back-reflection Laue pattern in (a). (c) Crystal growth direction (+) shown in stereographic projection, also determined from the pattern in (a).

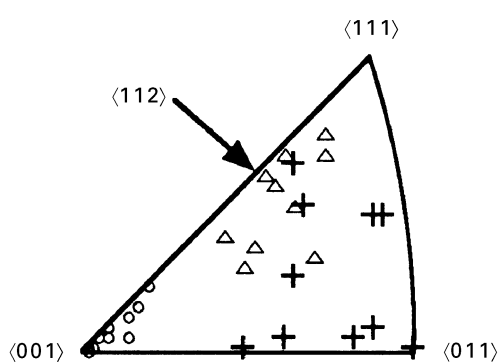


Figure 4 Crystallographic orientations of BSO single-crystal rods grown from the same platinum (+) seed 16.8 mm h^{-1} , (Δ) 68.8 mm h^{-1} , and (\circ) 106.8 mm h^{-1} .

angular displacement from the preferred orientation ($\langle 011 \rangle$, $\langle 112 \rangle$ or $\langle 001 \rangle$) decreases with increasing pulling rate. The crystallographic orientations of all ten crystal rods grown at 106.8 mm h^{-1} are exactly $\langle 001 \rangle$, or the orientations which deviate by less than 15° from $\langle 001 \rangle$. Furthermore, the crystallographic

orientations of all ten crystal rods produced at 106.8 mm h^{-1} appear to be nearly parallel to the crystal plane formed by $\langle 001 \rangle$ and $\langle 111 \rangle$.

3.4. Growth direction with BSO seed

Fig. 5a shows the growth direction (+) of a BSO crystal rod (2.28 mm diameter) grown from a platinum seed at 88.8 mm h^{-1} . By using this crystal rod as a seed, a BSO crystal rod (the same diameter as the seed) was grown at 16.8 mm h^{-1} . Its growth direction (*) is also shown in Fig. 5a. (The diffraction area was sampled from the new crystal rod which had been grown to 30 mm in length. Diffraction areas for the following experiments were selected in the same way.) There is no inclination of the growth direction in this state.

Fig. 5b shows the growth direction (+) of a BSO crystal rod (2.30 mm diameter) grown from a platinum seed at 106.8 mm h^{-1} . By using this crystal rod as a seed, a BSO crystal rod (with same diameter as the seed) was again grown at 106.8 mm h^{-1} , * in Fig. 5b.

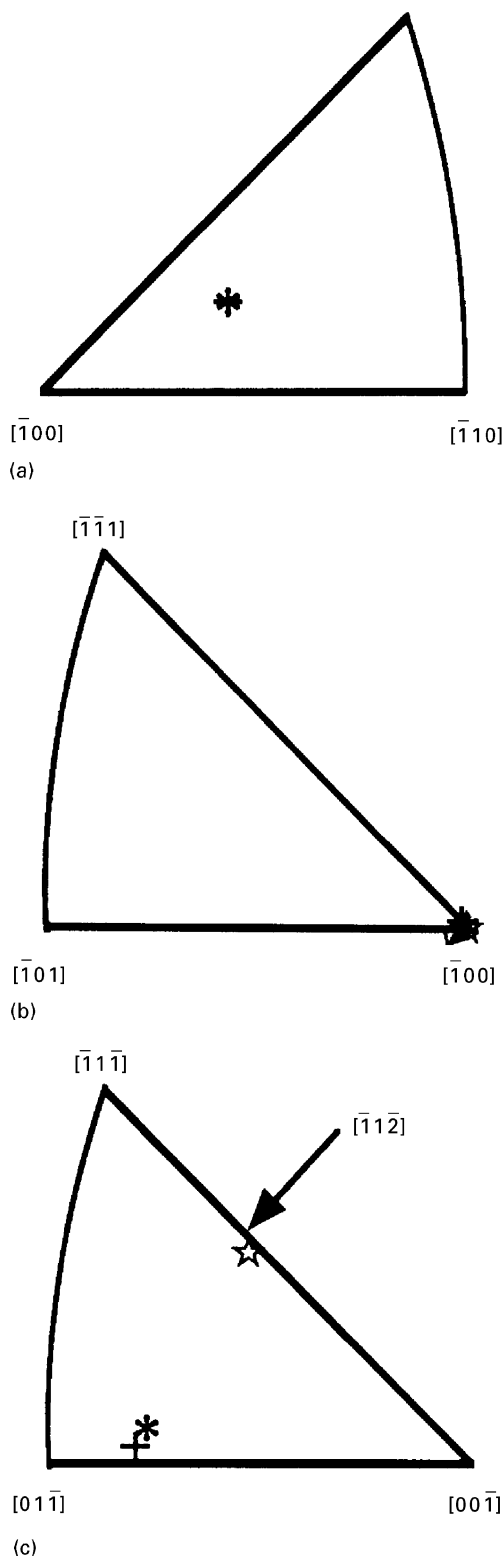


Figure 5 Summary of the results on inclinations of BSO growth directions. (a) (+) Orientation of the BSO crystal grown from a platinum seed at 88.8 mm h^{-1} . (*) Orientation of the BSO crystal grown at 16.8 mm h^{-1} from a crystal with orientation +. (b) (+) Orientation of the BSO crystal grown from a platinum seed at 106.8 mm h^{-1} . (*) Orientation of the BSO crystal grown at 106.8 mm h^{-1} from a crystal with orientation +. (★) Orientation of the BSO crystal grown at 16.8 mm h^{-1} from a crystal with orientation of *. (c) (+) Orientation of the BSO crystal grown from a platinum seed at 16.8 mm h^{-1} . (*) Orientation of the BSO crystal grown at 50.0 mm h^{-1} from a crystal with orientation of +. (★) Orientation of the BSO crystal grown at 106.8 mm h^{-1} from a crystal with orientation of +.

There is a very small inclination of the growth direction from the direction near (but not exactly) $\langle 001 \rangle$ ($[\bar{1}00]$) to exactly $\langle 001 \rangle$ ($[\bar{1}00]$). With Wulf's stereographic net, this angle of inclination was measured as only 1.1° . By using this new crystal rod as a seed, a BSO crystal rod (with the same diameter as a seed) was grown at 16.8 mm h^{-1} , (★ in Fig. 5b). There is no inclination of growth direction in this state.

Fig. 5c shows the growth direction (+) of the BSO crystal rod (2.31 mm diameter) grown from a platinum seed at 16.8 mm h^{-1} . By using this crystal rod as a seed, BSO crystal rods (with the same diameter as seed) were grown at 50.0 and 106.8 mm h^{-1} . Their growth directions are shown (*, ★, respectively) in Fig. 5c. With Wulf's stereographic net, the angles of inclination of the growth directions were measured as 2.5° (*) and 23.3° (★) relative to the seed orientation (+). These results show the growth direction of the produced BSO crystal rod inclined from a direction near $[01\bar{1}]$ to one near $[\bar{1}1\bar{2}]$ when the pulling rate was higher than 50.0 mm h^{-1} . The angle of inclination increases with the pulling rate.

The exact critical pulling rate for the inclination of the growth direction of the BSO crystal rod is difficult to determine owing to the limit in the accuracy of measuring crystal orientations. However, if different measurements were carried out for the same crystal rod, then an angle change as small as $\pm 0.15^\circ$ can be detected easily from the films of the Laue pattern. This is because the parallelism between the axis of the crystal rod and the film as well as the perpendicularity between the axis of the crystal rod and the inlet X-ray beam for different tested positions in the same crystal rod can be considered to be the same.

Fig. 6 shows three orientations measured from the same BSO crystal rod. The orientation shown by + is that of the BSO seed, which is the same as that shown in Fig. 5c. The orientation shown by \circ is that of the new BSO crystal produced with a pulling rate of 28.8 mm h^{-1} . The orientation shown by \bullet is that of the new BSO crystal produced with a pulling rate of 35.0 mm h^{-1} . There is no inclination of growth direction if the pulling rate is 28.8 mm h^{-1} or less, but about 0.8° if the pulling rate is 35.0 mm h^{-1} . Therefore, it can be estimated that the critical pulling rate for the inclination of the growth direction is about 30 mm h^{-1} .

3.5. Facet morphologies in different growth directions

The facet morphologies (here cross-section shapes) of the BSO single-crystal rods grown in three typical directions, $\langle 001 \rangle$, $\langle 011 \rangle$ and $\langle 111 \rangle$, are shown in Figs 7a, 8a and 9a, respectively. Figs. 7b, 8b and 9b are the theoretical facet morphologies of cubic crystals for growth directions along $\langle 001 \rangle$, $\langle 011 \rangle$ and $\langle 111 \rangle$, respectively. These three typical growth directions are shown by \circ in the centres. Small differences between the actual morphologies and theoretical ones may arise due to surface tension or the inversion of the morphological polarity [13]. The facet orientations in Figs 7a, 8a and 9a can be easily determined from the Laue patterns in Figs 7c, 8c and 9c. Here the inlet

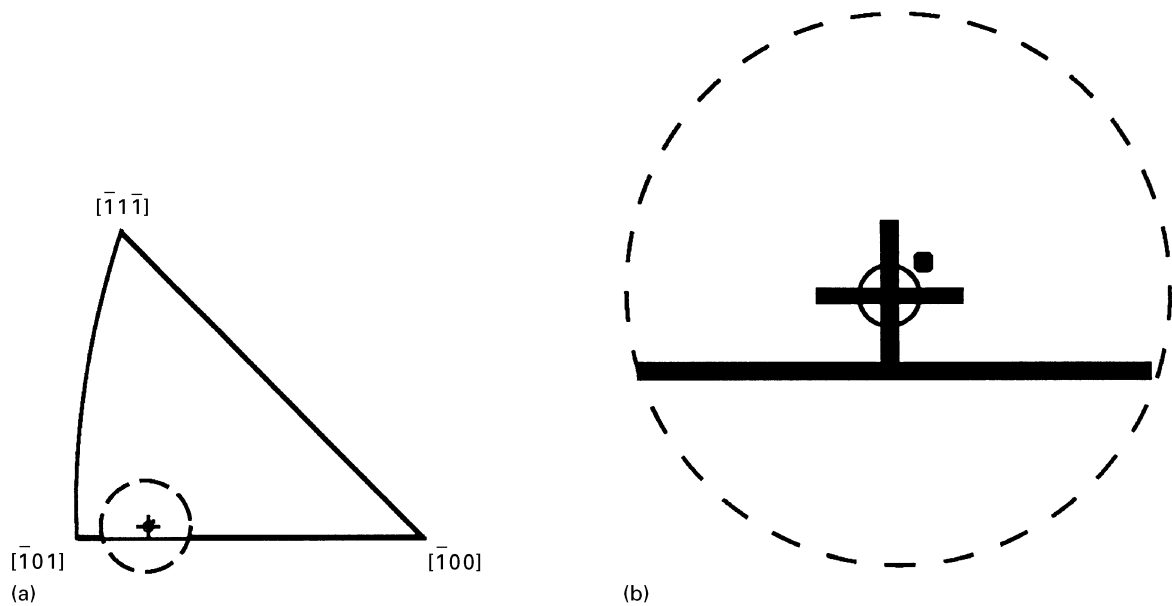


Figure 6 Determination of the critical pulling rate for the inclination of the growth direction. (a) (+) Copied from Fig. 5c, the orientation of a BSO crystal grown from a platinum seed at 16.8 mm h^{-1} . (○) The orientation of a BSO crystal grown at 28.8 mm h^{-1} from a BSO seed with the orientation shown by + in this figure. (●) The orientation of the BSO crystal grown at 35.0 mm h^{-1} from a BSO seed with the orientation shown by (○) in this figure. (b) Magnification ($\times 6$) of the area shown in (a).

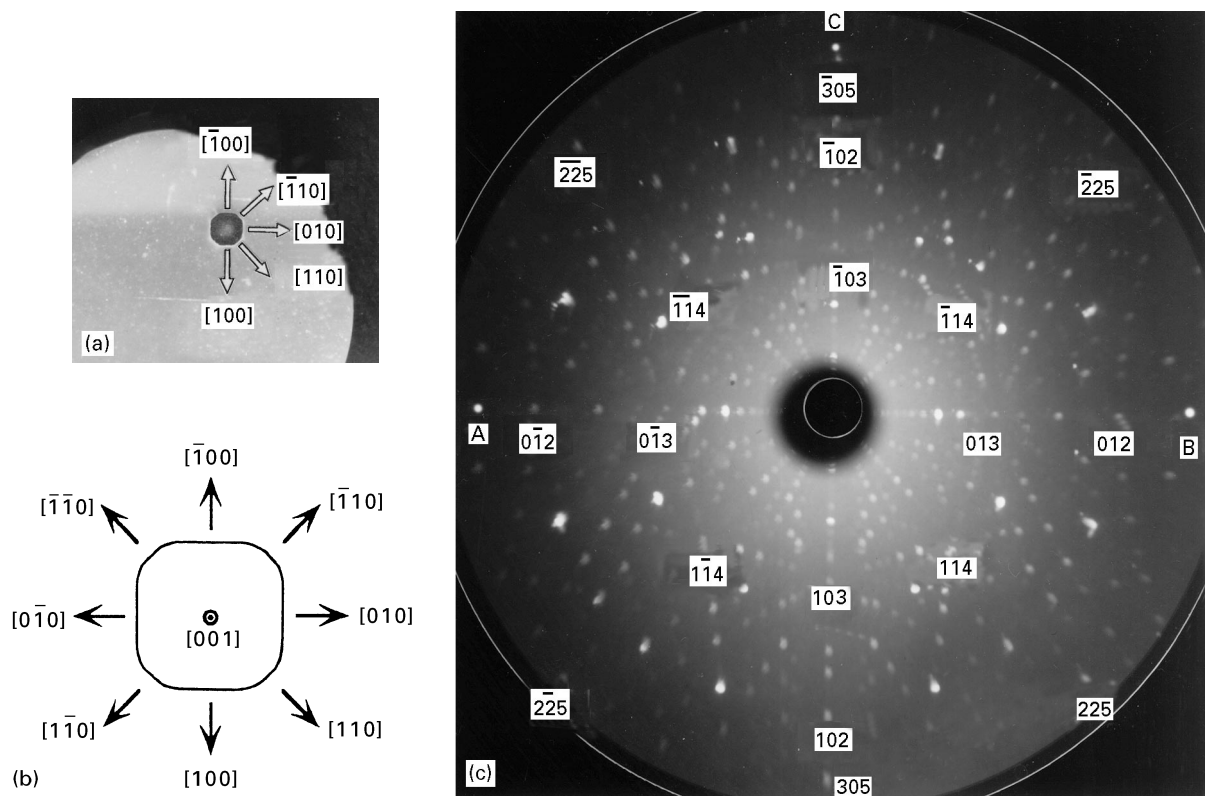


Figure 7 (a) Cross-section view of the facet morphology of BSO grown in the $\langle 001 \rangle$ direction. (b) Theoretical facet morphology of a cubic crystal rod grown in the $\langle 001 \rangle$ direction. (c) Back-reflection Laue pattern of the cross-section of BSO grown in the $\langle 001 \rangle$ direction.

X-ray beam was perpendicular to the cross-section of the crystal rod. Only five, three and seven normal vectors of the representative facets are indicated in Figs 7a, 8a and 9a. The others are similar to Figs 7b, 8b and 9b, respectively, and can be simply indicated by comparing geometric similarity between them. Both the facet morphologies in Figs 7a, 8a and 9a and the back-reflection Laue patterns in Figs 7c, 8c and 9c

show the tetrad-, diad- and triad-rotational symmetries of BSO crystal rods grown along $\langle 001 \rangle$, $\langle 011 \rangle$ and $\langle 111 \rangle$, respectively.

4. Discussion

The crystal growth rate is usually proportional to the temperature gradient [14, 15]. In the crystal growth

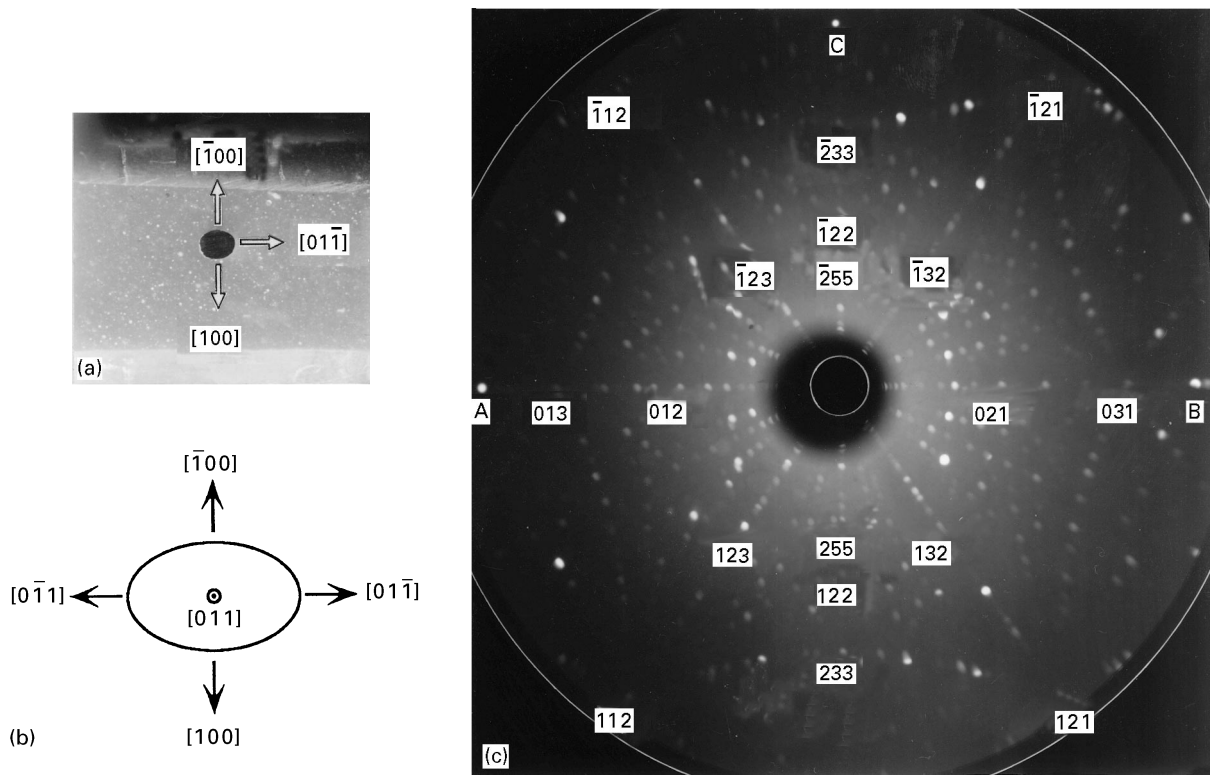


Figure 8 (a) Cross-section view of the facet morphology of BSO grown in the $\langle 011 \rangle$ direction. (b) Theoretical facet morphology of a cubic crystal rod grown in the $\langle 011 \rangle$ direction. (c) Back-reflection Laue pattern of the cross-section of BSO grown in the $\langle 011 \rangle$ direction.

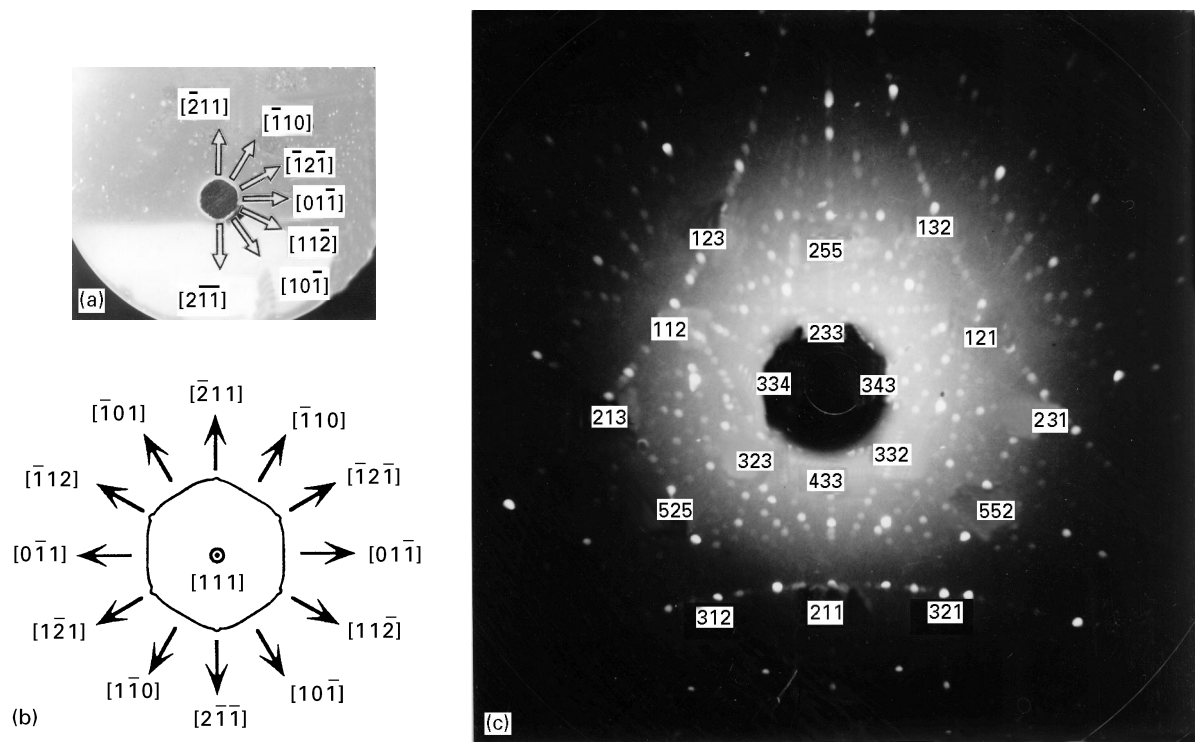


Figure 9 (a) Cross-section view of the facet morphology of BSO grown in the $\langle 111 \rangle$ direction (b) Theoretical facet morphology of a cubic crystal rod grown in the $\langle 111 \rangle$ direction. (c) Back-reflection Laue pattern of the cross-section of BSO grown in the $\langle 111 \rangle$ direction.

process by a floating zone, the latent heat of solidification is mostly transferred in the axial direction of the grown crystal rod rather than in a radial direction. Thus the temperature gradient in the axial direction is usually much larger than that in the radial direction, especially for a small diameter, such as those in the

present work. Therefore, the crystal growth rate is mostly controlled by the stacking rate of crystal planes perpendicular to the growth direction (i.e. the axial direction of the crystal rod).

The BSO crystal has a space group $I23$ [6]. The complex structure of BSO (due to multi-type atoms in

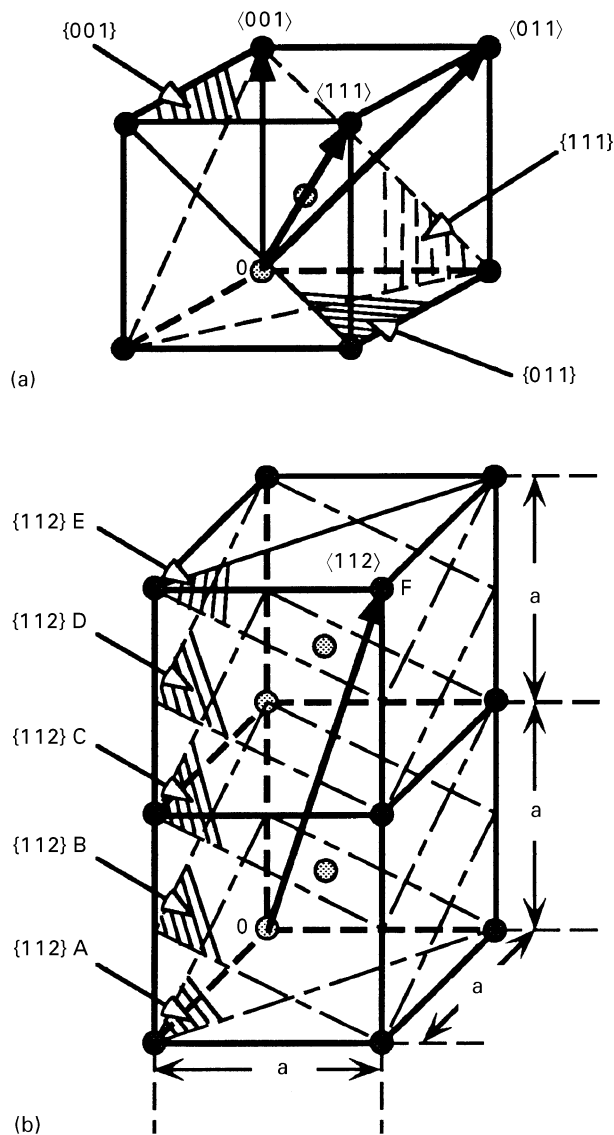


Figure 10 (a) Schematic representation of the BSO Bravais lattice with a bcc structure. (b) Schematic representations of the $\langle 112 \rangle$ crystal directions and $\{112\}$ crystal planes.

a unit cell) makes it difficult to relate its growth crystallography directly with its crystal structure. A simple explanation can be obtained from an analysis of its Bravais lattice (bcc), as shown in Fig. 10. The crystal planes $\{011\}$ are the closest-packed layers with a planar density of $\sqrt{2} \approx 1.414$ $\text{Bi}_{12}\text{SiO}_{20}$ molecules per a^2 , where a is the lattice constant. The planar densities of $\{001\}$, $\{111\}$ and $\{112\}$ crystal planes are 1, $\sqrt{3}/3 \approx 0.577$ and $\sqrt{6}/3 \approx 0.816$ $\text{Bi}_{12}\text{SiO}_{20}$ molecule per a^2 , respectively. Thus, the stacking rate for $\{011\}$ is the smallest if the numbers of crystallizable BSO molecules per unit time are the same. For a platinum seed, the orientation of the primary small crystal on the top of the platinum wire is arbitrary, if the diffusion rate of atoms in the melt and the crystallization rate are much higher than the pulling rate, then both dense crystal planes such as $\{011\}$ and non-dense crystal planes such as $\{001\}$, $\{111\}$ or $\{112\}$ can develop equally. This results in a large angular displacement from the preferred orientation ($\langle 011 \rangle$) for low pulling rates. On the other hand, because both the dense crystal planes and the non-dense crystal

planes can develop fully under a low pulling rate, the growth rate in a direction with a larger distance between crystal planes, such as $\langle 011 \rangle$, may become higher if the stacking rates for all crystal planes are not much different. This makes the crystal growth in a direction near $\langle 011 \rangle$ slightly more preferable than that in a direction near $\langle 001 \rangle$ if the pulling rate is very low, as shown in Fig. 4. With increasing pulling rate, a growth of the non-dense crystal planes such as $\{001\}$, $\{111\}$ or $\{112\}$ become preferable due to their higher stacking rate. The stacking orders of $\{001\}$, $\{111\}$ and $\{112\}$ are ABABAB, ABCABCABC and ABCDEFABCDEF, respectively. The simplest stacking order of $\{001\}$ crystal planes results in the preferred growth direction being near $\langle 001 \rangle$ if the pulling rate is as high as 106.8 mm h^{-1} (Fig. 4). By the same analysis, the inclinations of the growth directions as shown in Fig. 5 can also be understood. However, it appears to be difficult to compare the stacking rates between $\{111\}$ and $\{112\}$ only by the Bravais lattice, although the experimental results in Figs 4 and 5 clearly show that the growth in $\langle 112 \rangle$ is more preferred than that in $\langle 111 \rangle$. A recent report on the morphology of BGO crystals grown along the $\langle 111 \rangle$ directions by the Czochralski method [16] revealed its complexity, non-identity, and growth-rate dependence. It may be this reason which makes the growth in $\langle 111 \rangle$ more difficult than that in $\langle 112 \rangle$, because BSO has a structure similar to BGO. This requires a further investigation to relate it to the practical crystal structure.

As shown in Section 3.4, inclination of the growth direction arose only if the pulling rate was over 30 mm h^{-1} . The angle of inclination of the growth direction increases with the pulling rate. When a platinum wire was employed as seed, the growth direction showed a clear preference only if the pulling rate was high (about 68.8 mm h^{-1} according to Fig. 4). The preference of the growth direction also increases with the pulling rate. The pulling rate in Czochralski growth for BSO is only $3\text{--}5 \text{ mm h}^{-1}$ [17] due to the small temperature gradient. This pulling rate is much smaller than the critical value for the inclination of the growth direction, 30 mm h^{-1} , as described above. Therefore, there is no inclination of the growth direction in the Czochralski process. The growth direction from a platinum seed can also be expected to be arbitrary. Thus the inclination or preference of the growth direction in producing BSO crystals has not hitherto been reported. In the floating zone growth process, the large temperature gradient allows a single crystal be produced at a very high pulling rate [8, 18]. Thus the inclination of the growth direction in the floating zone growth process becomes possible, as shown in the present work. The characteristics of inclination and preference of the growth direction may be useful in allowing the choice of a suitable orientation of the grown crystal rod or fibre to obtain the best properties.

5. Conclusions

1. The crystallographic orientation of the BSO single-crystal rod grown from a platinum seed is

related to the pulling rate. Statistically, the probability of the growth direction being near $\langle 011 \rangle$ appears to decrease with the increase in the pulling rate higher than 30 mm h^{-1} . The probability of a growth direction near $\langle 112 \rangle$ appears to be highest if the pulling rate is moderate (about 68 mm h^{-1}), and that of one near $\langle 001 \rangle$ appears to be highest if the pulling rate is more than 100 mm h^{-1} or so. The angular displacement from the preferred orientation ($\langle 011 \rangle$, $\langle 112 \rangle$ or $\langle 001 \rangle$) decreases with the increase of the pulling rate. The orientations of all BSO single-crystal rods produced at 106.8 mm h^{-1} are wholly $\langle 001 \rangle$ or deviate by less than 15° from $\langle 001 \rangle$.

2. With a BSO crystal seed, the produced BSO crystal rod has the same orientation as the seed crystal if the pulling rate is less than 30 mm h^{-1} . For higher pulling rates, however, the growth direction of the new BSO crystal rod is dependent on the following conditions. For $\langle 001 \rangle$ BSO seed, the growth direction of the produced BSO crystal rod is also $\langle 001 \rangle$. For BSO seed with an orientation near $\langle 011 \rangle$ or $\langle 111 \rangle$ but far from $\langle 001 \rangle$, the growth direction inclines first to $\langle 112 \rangle$ although there is a slight inclination to $\langle 001 \rangle$ in the same process. For BSO seed with an orientation near $\langle 001 \rangle$ but far from both $\langle 011 \rangle$ and $\langle 111 \rangle$, the growth direction inclines mostly to $\langle 001 \rangle$.

3. The facet morphology of the BSO single-crystal rod is related to its growth direction. The cross-section of BSO single-crystal rod grown along $\langle 001 \rangle$ is an octagon with tetrad-rotational symmetry, that grown along $\langle 011 \rangle$ is an ellipsoid with diad-rotational symmetry, and that grown along $\langle 001 \rangle$ is a hexagon with triad-rotational symmetry. The cross-sections of the

BSO single-crystal rods grown in other directions are not regular, because there is no clear symmetry.

References

1. A. E. ATTARD, *J. Appl. Phys.* **71** (1992) 933.
2. J. KHOURY, M. CRONIN-GOLOMB and C. WOODS, *ibid.* **77** (1995) 7.
3. M. T. HARRIS and J. J. BLARKIN, *Appl. Phys. Lett.* **60** (1994) 2162.
4. S. L. SOCHAVA, K. BUSE and E. KRÄTZIG, *Phys. Rev. B* **51** (1995) 4684.
5. C. LIN and S. MOTAKEF *J. Cryst. Growth* **128** (1993), 834.
6. National Bureau of Standards (US) "Powder Diffraction File" (compiled by the Joint Committee on Powder Diffraction Standards (JCPDS)) **37** (International Centre for Diffraction Data (ICDD) 1987) no. 485.
7. T. TAKAMORI and J. J. BOLAND, *J. Mater. Sci. Lett.* **10** (1991) 972.
8. S. FU and H. OZOE, *J. Appl. Phys.* **77** (1995) 5968.
9. A. J. C. WILSON, "International Tables for Crystallography", Vol. C (The Kluwer Academic, Netherlands, 1992).
10. S. FU and H. OZOE, *J. Phys. Chem. Solids* **57** (1996) 1269.
11. S. FU and H. OZOE, *J. Mater. Res.* **11** (1996) 2575.
12. A. B. GRENINGER, *Z. Kristallogr.* **A91** (1935) 424.
13. X. XU, J. LIAO, B. SHEN, X. CHEN and C. HE, *J. Cryst. Growth* **134** (1993) 337.
14. K.-TH. WILKE, "Kristall Züchtung" (Thun, Harri Deutsch, Frankfurtam Main, 1988) p. 303 (in German).
15. S. FU and H. XU, *J. Phys. Condens. Matter* **4** (1992) 8303.
16. M. T. SANTOS, C. MARÍN and E. DIÉGUEZ, *J. Cryst. Growth* **160** (1996) 283.
17. D. KRISHNAMURTHY, R. GOPALAKRISHNAN, D. ARIVUOLI and P. RAMASAMY, *J. Mater. Sci. Lett.* **12** (1993) 1218.
18. S. FU, J. JIANG, J. CHEN and Z. DING, *J. Mater. Sci.* **28** (1993) 1659.

Received 7 May 1996

and accepted 7 January 1997